RADIATION-RESISTANT DEVICE PHENOMENA

By William C. Follmer and Walter M. Kane

February 1965

Prepared Under Contract No. NASW-997 by

PHILCO CORPORATION
A Subsidiary of Ford Motor Company
Applied Research Laboratory
Blue Bell, Pennsylvania

NATIONAL AERONAUTICS AND SPACE ADMINISTRATION

TABLE OF CONTENTS

Section	Page
SUMMARY	1
INTRODUCTION	2
FACILITY DETAILS	3
Vacuum System and Drybox Unit	3
Oxygen Pressure Monitor and Controller	3
Changes and modifications	3
Operational procedure	4
System performance	4
Resonant Quartz Microscale Deposition-Rate Monitor and Controller	5
Systems modifications and changes	5
Operational procedure	5
System performance	6
ALUMINUM-OXIDE FILMS	7
Evaporation Technique	7
Evaporator structures	7
Distribution of evaporant	7
Oxide Film Production	9
Electrical Test Data	9
General notes	9
Test results	9

TABLE OF CONTENTS (Cont)

Section		Page
	Variation of parameters with time and ambient	15
	Dependence of Electrical Properties on σ	15
	Variation of C with σ	15
	Variation of r_{ac} with σ	20
ELECTRON TRANSPORT THROUGH THIN FILMS		23
	Introduction	23
	Diode Preparation	23
	Transport Experiment	26
ABSTRACT		35

LIST OF ILLUSTRATIONS

Figure		Page
1	Crucible With Basket Heater (lower photo) and a Sauereisen 8-Bonded Basket Heater	8
2	Aluminum-Oxide Evaporation Pattern With Radiation Shield	10
3	Capacity Versus Time for Run A-1	16
4	R_{dc} Versus Time for Run A-1	17
5	r_{ac} Versus Time for Run A-1	18
6	$\frac{T}{\epsilon_f}$ Versus σ for Small-Area Samples	19
7	$r_{ac}A$ Versus σ, Small Area, for Runs A-1 to A-5	21
8	Simplified Energy Diagram of Collector Diode	24
9	Gold-Silicon Diode	25
10	I-V Curve of Au-Si Diode	27
11	I-V Curves, Showing Isolation of Land Areas From Silicon Surface by SiO_2	27
12	I-V Characteristics of Au-Si Diode	28

Appendix		Page
A	Operation and Performance of the R.Q.M. Deposition Monitor and Controller	30

SUMMARY

24295

The energetic electron transport experiment has been severely hampered by unexpected difficulties with the electron gun structure described in the First Quarterly Report. After the gun assembly was cleaned and reinstalled in the vacuum chamber, it was impossible to obtain any electron current to the sample. The cause of this malfunction is not known. In addition, the very large area (1 sq. cm) collector diode has an unusually large saturation current density. This excess current further degrades the signal-to-noise ratio expected when a transport measurement is attempted. The oxide shorting problem has been eliminiated by changing the processing steps used to apply the ohmic contact and isolated land areas.

The facilities required for controlled production of reactively evaporated aluminum-oxide films are now complete and a number of controlled deposition runs have been made. Highly insulating aluminum-oxide films ranging in thickness from 10 to 40 $\mu gm\ cm^{-2}$ have been prepared. The yield has been consistently high even for the thinnest samples. These films exhibit a time variation in their electrical properties while being stored in a dry-nitrogen ambient. Upon exposure to atmosphere, there is a transient decrease in film impedance. At the present time this is thought to be due to the effects of atmospheric water vapor.

Author

INTRODUCTION

The metal-base transistor (MBT) approach to a radiation-resistant active device requires that one obtain a thin metallic film whose thickness is considerably less than the mean free path of the injected electrons. The electron transport experiment was designed to obtain the desired information on electron mean free path by providing a beam of low-energy electrons which were to be collected by a metal semiconductor diode. By determining the fraction of the total beam current which, after passing through the metal film, flows through the surface-barrier diode as the incident beam energy is varied, one can experimentally determine the attenuation length of the injected electrons as a function of their excess energy.

In addition to the electron transport experiment, equipment and facilities have been completed for the production of thin insulating films of aluminum-oxide produced by the reactive evaporation of aluminum. The deposition process is controlled by a resonant quartz microscale deposition rate control unit designed and constructed at this laboratory. This unit utilizes the frequency shift of a resonant quartz crystal when the material is deposited on one of the faces. This frequency shift is monitored and produces the electronic signals that control the deposition. The aluminum-oxide films are obtained by the slow evaporation of aluminum in a partial pressure of oxygen of a few times 10^{-4} mm hg. The resulting dielectric film is sandwiched between two metal electrodes and its properties as an insulator are being extensively studied.

FACILITY DETAILS

Vacuum System and Drybox Unit

With the completion of the items described later in this section, the vacuum system and drybox assembly is now complete and operating very satisfactorily.

The absolute filter and recirculating unit has been installed on the drybox. This unit should further reduce the possiblity of film contamination by submicron dust particles. The sliding armport leak was sealed by a vinyl gasket and aluminum supporting channel. The vinyl gasket is cemented to the original sealing area on the sliding arm panel. This gasket then slides in the aluminum channel. The seal between the gasket and the aluminum channel is due to small extrusions in the outer surface of the vinyl gasket which produce a high local pressure and a very satisfactory seal.

A vacuum line has been installed in the drybox to operate a vacuum tweezer that is used for handling the substrates. In addition, the vacuum line provides for a suction pickup that is used to clean the interior of the drybox if it becomes accidentally contaminated.

To facilitate electrical tests in the dry-nitrogen environment of the drybox, a micromanipulator probe assembly has been installed in the drybox. Coaxial feedthroughs have also been installed to provide electrical connections to the external test instruments.

A nitrogen pressure of 0.3 inch of water is maintained in the drybox during all operations. Under standby conditions, the pressure is reduced to 0.05 inch of water to conserve the nitrogen gas supply.

Oxygen-Pressure Monitor and Controller

Changes and modifications. - To vent the leak valve and solenoid valve assembly, a double-pole, double-throw switch was installed in place of S_2 (Figure B-2, page 23, First Quarterly Report, December 1964). This switch now has an additional spring-return position which permits the solenoid valve to be held open with the ionization gauge off. In this manner the solenoid valve and leak valve can be flushed with oxygen prior to the actual deposition run.

In this particular system, C_1 (Figure B-2, First Quarterly Report) was determined experimentally to be 47 microfarads.

Operational procedure. - Assuming that one has the system under vacuum, the operational procedure for using the oxygen-pressure regulator is as follows: With the main AC switch "On," the MODE switch in "Manual," and the ionization gauge "Off" (standby), the SOLENOID VALVE switch is held in the "Vent" position for approximately 1.0 minute to allow oxygen flow to flush the system. The ionization gauge and pressure recorder are then turned on and set to the desired pressure range (typically, 10^{-4} range). The SOLENOID VALVE is then switched to the "Open" position. The resulting pressure burst will usually trip the overload on the ionization gauge; however, the gauge is reset repeatedly until it remains on scale. With the gauge unit reading on scale, the PRESSURE SET dial (R_1, Figure B-2, First Quarterly Report) is set to the desired value. The MODE switch is then switched to "Automatic" and the servo system will then vary the leak-valve setting to obtain the preset pressure. Note that in the "Manual" position of the MODE switch the leak valve is operated by the spring-return INCREASE-DECREASE switch. At any time during the run, the oxygen pressure may be varied by simply readjusting R_1 (Figure B-2, First Quarterly Report) to the new pressure desired.

At the termination of the run, the MODE switch is returned to the "Manual" position and the system pressure reduced with the MANUAL switch to a level below 5×10^{-4}. This is done to reduce the initial pressure burst when starting up the system. The SOLENOID VALVE is now "Closed" and the oxygen flow shut off. One can then proceed with the remainder of the process.

System performance. - The pressure-control system maintains the indicated pressure to better than 1-percent accuracy. The response speed of the system is limited to the maximum value that is compatible with the pumping speed and typically requires 30 seconds to come within 1 percent of the final value.

The pressure-control system is capable of operation at any pressure where a suitable leak valve can be fabricated. The present unit is satisfactory for system pressures greater than 1×10^{-4} mm hg.

Resonant Quartz Microscale (R.Q.M.) Deposition-Rate Monitor and Controller

Systems modifications and changes. - Experimentally, the damping capacitor, C_6 (Figure C-12, First Quarterly Report), has been determined to have an optimum value of 80 microfarads for the aluminum-oxide crucible evaporator. During subsequent evaporation runs, there has been no tendency toward system oscillations with the servo gain such that the average variation in deposition rate is held to less than 1 percent.

To improve the mixer waveform, R_6 (Figure C-11, First Quarterly Report) has been changed to 680 ohms and is now connected from the base of Q_2 to ground.

Operational procedure. - A summary of the operational procedure is covered in the following paragraphs, and the detailed operational procedure is contained in Appendix A.

In operating the R.Q.M., one must first determine the desired mass per unit area of the deposit and the desired mass deposition rate. With these two parameters known, one then calculates the correct frequency-meter setting and the DIFFERENTIATOR MULTIPLIER, RATE PROGRAMMER MULTIPLIER, and RATE SET settings. The controls are then set at the proper values. With the system under vacuum and all the equipment operating with the MODE switch in the "Manual" position, the evaporator is heated to approximately the correct temperature by adjusting the MANUAL VARIAC. The sample oscillator is then exposed and the RATE DETECTOR switched "On." Under manual control the evaporator voltage is adjusted with the MANUAL VARIAC until the deposition rate as read on the rate recorder is at approximately the desired value. The system is then switched to "Automatic" with the MODE switch. In the "Automatic" position, the servo-driven variac will automatically vary the evaporator voltage to maintain the deposition rate at the preset value. The shutter, which up to this point has protected the substrate from the evaporant, is then opened to allow the evaporant to be deposited on the substrate. When the desired mass per unit area of evaporant has been deposited on the substrate, as read on the mass recorder, the shutter is closed over the substrate, cutting off the deposition. The system is then switched to "Manual" control and the evaporator power reduced to zero. This effectively concludes the evaporation run. The RATE DETECTOR is then shut "Off" to protect the differentiator circuit from any subsequent transients.

System performance. - Detailed performance limits of this system are also covered in Appendix A. The following is a summary of the performance characteristics applicable to the aluminum-oxide deposition.

Deposition rates of 4×10^{-8} grams cm^{-2} sec^{-1} have been used for all the aluminum-oxide runs to date. The average deposition rate is held to the preset value with an error of less than 1 percent for periods of greater than 1.0 minute. A fluctuation in evaporation rate of plus or minus 3 percent is thought to be caused by the random evaporation from the source and the thermal effects resulting from the aluminum-oxygen reaction at the crystal surface. Aluminum-oxide films ranging from 2 to 40 micrograms cm^{-2} have been successfully deposited at a constant deposition rate.

ALUMINUM-OXIDE FILMS

Evaporation Technique

Evaporator structures. - Four evaporator structures have been examined: the tungsten boat, a conical tungsten basket, a tungsten coil, and an aluminum-oxide crucible. In all cases the exposed tungsten was rapidly attacked by the molten aluminum and was not suitable for extended runs. The aluminum-oxide crucible was not attacked by the molten aluminum, so all successful evaporations have been carried out using an aluminum-oxide crucible. The crucible has been heated with a commercial radiation heater, a tungsten basket, and a tungsten basket bonded to the crucible with Sauereisen. As expected, the radiation heater had a rather long time constant, and it was difficult to slow the servo-system response sufficiently to eliminate the oscillation problem.

The tungsten basket heater had a much faster response time and, in addition, required considerably less heater power; therefore, this unit was used in the majority of experimental runs. Initial experiments with a Sauereisen-bonded basket heater produced and unexplainable black deposition on the evaporation shields. Because of the unknown contamination thus produced, device runs were made with the unbonded basket heater. The Sauereisen-bonded heater will be investigated more thoroughly using a different Sauereisen compound which the manufacturer claims will eliminate the contamination problem. The desire to use the bonded basket heater results from the reduction of the heater power by an order of magnitude and a corresponding increase in the response speed. The lower heater power reduces the in-vacuum system heat and allows longer runs to be made. Increasing the response speed alleviates the problem of deposition-system oscillation. Figure 1 is a photograph of the oxide crucible with a basket heater and a Sauereisen 8-bonded basket heater.

Distribution of evaporant. - Several aluminum-oxide runs were made using glass substrates with a completely open mask. The oxide film was sandwiched between two semitransparent aluminum films. The color variations over the surface of the resulting interference filter are an indication of the uniformity of the oxide film. Initial runs indicated a substantial variation in thickness. This variation was corrected by increasing the diameter of the aperture in the radiation shield and by moving the crucible closer to the radiation shield. The resulting evaporation pattern was determined by placing a 10-cm-square glass substrate in the position

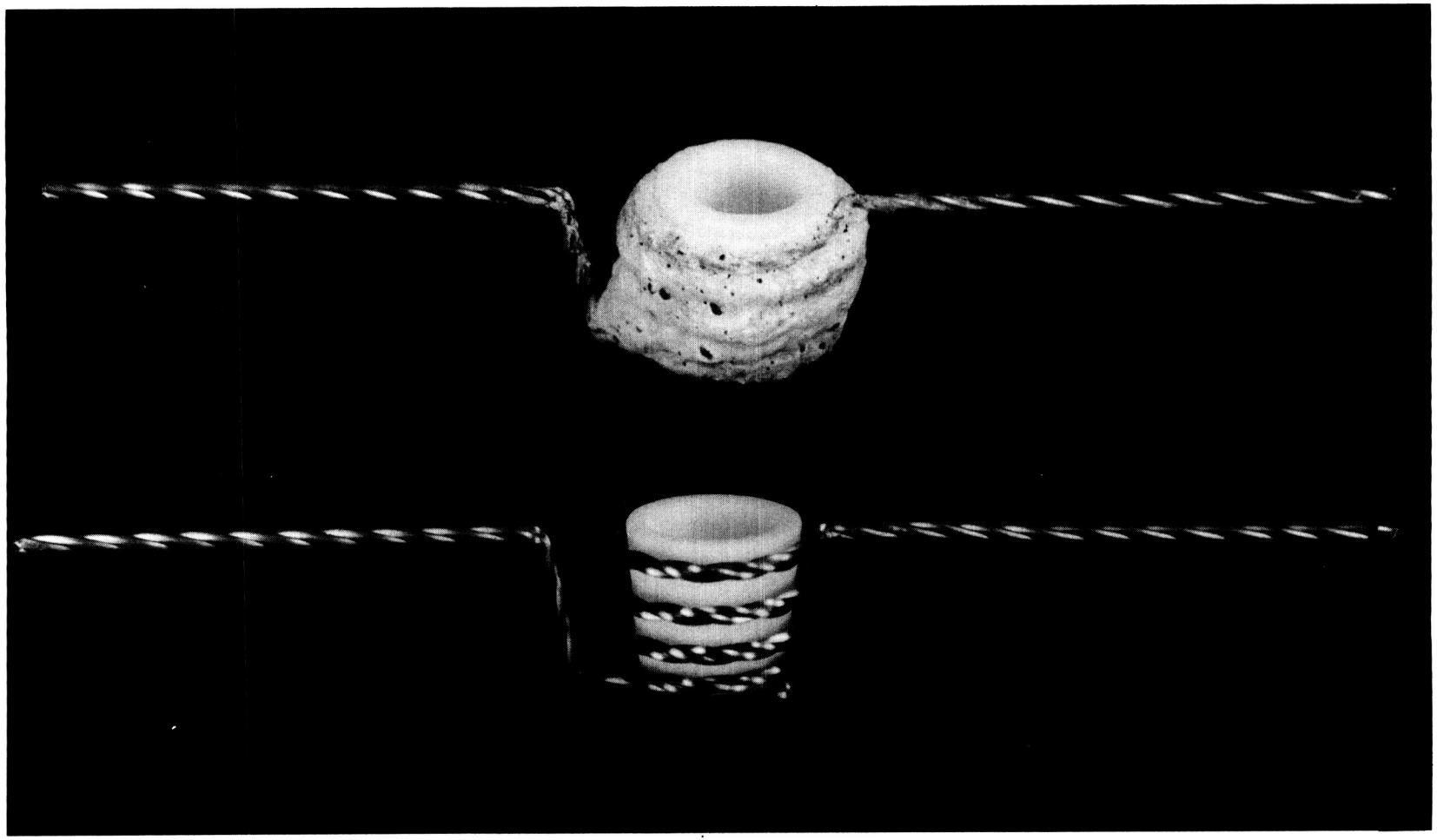

Figure 1. Crucible With Basket Heater (lower photo) and a Sauereisen 8-Bonded Basket Heater

normally occupied by the sample oscillator and substrate. Aluminum was evaporated from the crucible onto the large glass substrate until it was nearly opaque. A microdensitometer was then used to obtain the optical density as a function of position. Since at low transmission (corresponding to high optical density) the optical density of a metal film is proportional to thickness, the resulting optical density curves are a good indication of relative thickness. The measurements of optical density have indicated that variations in thickness are now limited by the geometry of the aluminum-oxide crucible and can be improved only by essentially flattening the crucible to eliminate shadowing caused by the walls of the crucible. Figure 2 is a polar plot of the thickness distribution as measured using this technique, with the relative positions of the sample oscillator and substrate indicated.

Oxide Film Production

Five aluminum-aluminum oxide-aluminum runs have been made. Each run consists of four small-area and four large-area capacitors which are formed simultaneously on the glass substrate. The samples were prepared by first depositing a base electrode of aluminum 25 micrograms cm^{-2} thick. The substrate was then installed in a second mask and aluminum oxide was reactively deposited. During the entire sequence of Al_2O_3 runs, the oxygen pressure was held at 8.4×10^{-4} mm hg and the deposition rate was maintained constant at 4×10^{-8} grams cm^{-2} sec^{-1}. The oxide surface mass for each run was varied by controlling the exposure to obtain oxide samples of 5, 10, 20, 30, and 40 micrograms cm^{-2}. The substrate and samples were then removed from the vacuum system and installed in the third mask, and counterelectrodes consisting of 25 micrograms cm^{-2} of aluminum were vacuum deposited. During the entire process, the samples and substrates were handled in the dry-nitrogen atmosphere provided by the drybox.

Electrical Test Data

General notes. - All the capacity samples were tested in the drybox and in air for dc leakage, using a Keithley Model 610A electrometer; and at 100 kc, the complex admittance was measured with a Boonton capacitance bridge.

Test results. - Details of the initial test results taken just after fabrication are summarized in Table 1. The data obtained after 1 day in air is summarized in Table 2.

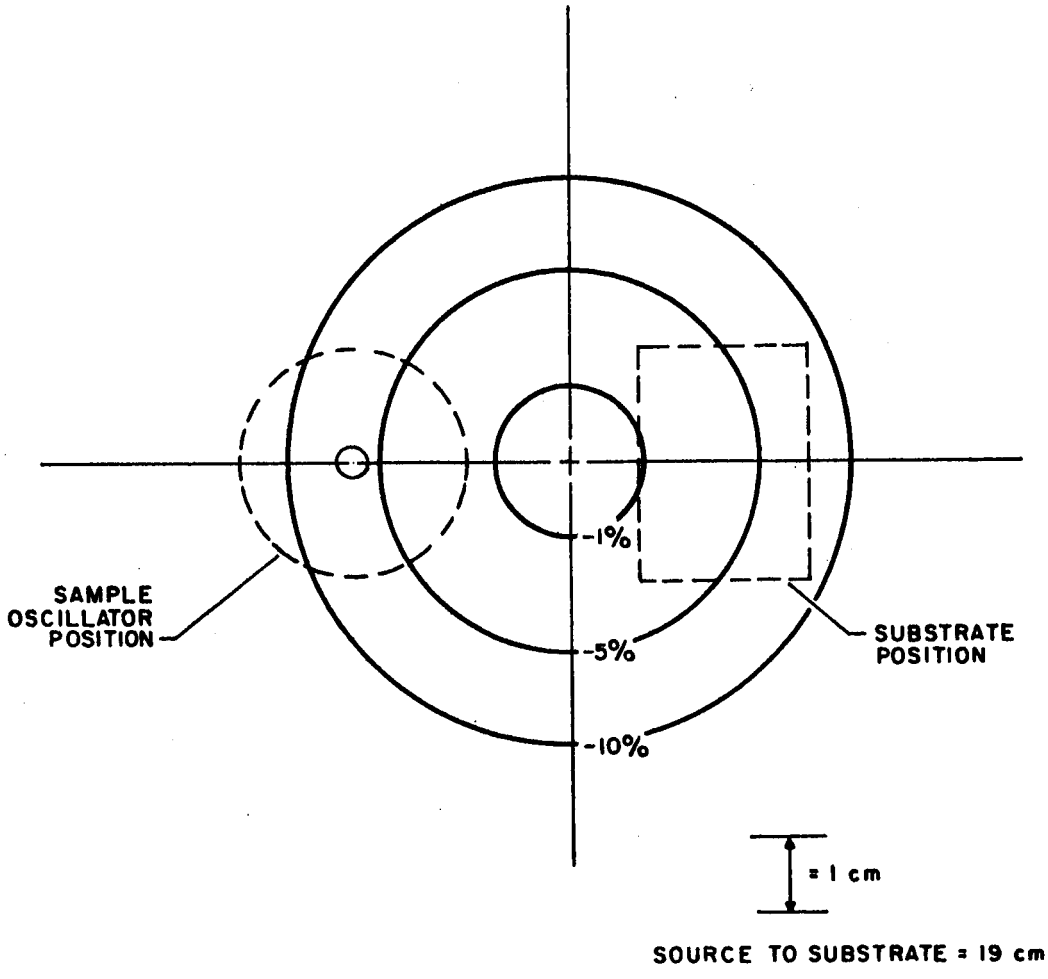

Figure 2. Aluminum-Oxide Pattern With Radiation Shield

Table 1. Device Data in N_2

Run	Sample	σ (μgm cm^{-2})	C (pf)	r_{ac} (10^6 ohms)	R_{dc} (ohms)
A-1	1	41.0	61.6	2.45	5.5×10^9
	2		63.0	2.42	5.7×10^9
	3		58.7	2.79	5.6×10^9
	4		61.9	2.04	5.5×10^9
	7		279.8	0.364	7.4×10^8
	8		287.1	0.398	7.2×10^8
	9		282.1	0.380	7.4×10^8
	10		292.8	0.364	7.4×10^8
A-2	1	30.0	85.0	1.74	$> 10^{12}$
	2		87.3	1.62	$> 10^{12}$
	3		83.6	1.54	$> 10^{12}$
	4		83.6	1.78	$> 10^{12}$
	7		398.7	0.164	6.5×10^5
	8		407.1	0.208	6.4×10^9
	9		394.4	0.221	6.3×10^9
	10		413.5	0.198	5.2×10^9
A-3	1	20.0	135.0	0.616	4.1×10^{10}
	2		131.8	0.834	6.1×10^{10}
	3		133.2	0.57	5.3×10^{10}
	4		130.8	0.69	6.6×10^{10}
	7		595.3	0.11	2.4×10^{10}
	8		642.0	0.083	2.1×10^{10}
	9		595.7	0.116	2.8×10^{10}
	10		602.3	0.022	2.9×10^4
A-4	1	10	316.2	0.52	$> 10^{12}$
	2		324.0	0.53	$> 10^{12}$
	3		306.6	0.54	$> 10^{12}$
	4		311.0	0.62	$> 10^{12}$
	7		Short		
	8		Short		
	9		1,443	0.055	8.6×10^{11}
	10		1,496	0.045	10.0×10^5

Table 1 (Continued)

Run	Sample	σ (μgm cm^{-2})	C (pf)	r_{ac} (10^6 ohms)	R_{dc} (ohms)
A-5	1	5.2	Short		
	2	↓	555.5	0.29	1.0×10^9
	3		519.5	0.33	$> 10^{12}$
	4		538.7	0.34	$> 10^{12}$
	7		2,461	0.032	$> 10^{12}$
	8		2,573	0.0275	6.4×10^{11}
	9		Short		
	10		2,643	0.0275	$> 10^{12}$

Table 2. Device Data, 1 Day in Air

Run	Sample	σ (μgm cm^{-2})	C (pf)	r_{ac} (10^6 ohms)	R_{dc} (ohms)
A-1	1	41.0	84.8	0.46	7.0×10^7
	2		86.4	0.46	7.1×10^9
	3		80.8	0.49	7.3×10^9
	4		80.8	0.59	7.4×10^9
	7		Short		
	8		400.0	0.085	8.3×10^8
	9		385.0	0.098	8.6×10^8
	10		405.0	0.082	8.4×10^8
A-2	1	30.0	116.2	0.362	6.1×10^9
	2		116.1	0.41	5.9×10^9
	3		109.6	0.42	6.1×10^9
	4		113.0	0.40	6.3×10^9
	7		525.0	0.066	6.0×10^6
	8		545.0	0.065	1.0×10^{10}
	9		521.6	0.07	8.8×10^8
	10		541.5	0.068	8.7×10^8
A-3	1	20.0	180.4	0.203	5.8×10^9
	2		182.5	0.208	5.8×10^9
	3		174.2	0.208	6.6×10^9
	4		176.0	0.219	5.6×10^9
	7		829.0	0.025	6.9×10^8
	8		856.5	0.285	7.0×10^8
	9		829.5	0.033	6.1×10^8
	10		846.2	0.0178	3.7×10^4
A-4	1	10.0	316.7	0.174	7.0×10^9
	2		307.2	0.208	6.7×10^9
	3		311.6	0.178	5.5×10^9
	4		290.0	0.225	7.3×10^9
	7		Short		
	8		Short		
	9		1,487	0.02	7.0×10^8
	10		1,552	0.0174	2.7×10^6

Table 2 (Continued)

Run	Sample	σ (μgm cm^{-2})	C (pf)	r_{ac} (10^6 ohms)	R_{dc} (ohms)
A-5	1	5.0	Short		
	2		568.0	0.085	7.8×10^8
	3		538.0	0.09	9.6×10^8
	4		553.0	0.08	5.1×10^9
	7		2,542	0.01	7.0×10^8
	8		2,631	0.0085	7.2×10^8
	9		Short		
	10		2,715	0.007	6.6×10^8

Variation in parameters with time and ambient. - Figures 3, 4, and 5 are plots of capacitances, dc leakage, and ac resistance as a function of time for a typical run. Note that the dc and ac losses increase smoothly while the sample is in the nitrogen atmosphere and increase rapidly to a higher value when the samples are exposed to air. The capacitance of the samples, as shown in Figure 3, varies in a similar manner, increasing smoothly while the sample is in a drybox and increasing rapidly to a higher value when the sample is exposed to air. This is similar to what has been reported previously[1] and is believed to be the result of water vapor absorption in the oxide.

Dependence of Electrical Properties on σ

Variation of C with σ. - If one plots $\frac{\epsilon_o A}{C}$, the area per unit capacity, versus the surface mass, σ, the slope of the resulting curve is $\frac{1}{\rho \epsilon}$, where ρ is the density of the material and ϵ is the relative dielectric constant. This slope is a measure of how close one approaches the bulk properties of the material. Figure 6 is such a plot for runs A-1 to A-5. Included in Figure 6 is the line corresponding to randomly oriented bulk sapphire assuming, $\rho = 3.97$ and $\epsilon = 9.25$.[2] Note that the $\rho\epsilon$ product is substantially larger than for the thin-film samples. The negative σ intercept of one microgram cm^{-2} is also interesting in that it is equivalent to the natural oxide formed on an exposed aluminum film. This is quite in agreement with the experimental use of an aluminum base electrode which may be expected to oxidize during its subsequent exposure to oxygen in the vacuum system prior to the oxide-film deposition.

By making measurements of the film thickness using a multiple-beam interferometer, it should be possible to deduce independent values for ρ and ϵ.

---

1. Da Silva, E. M. and White, P., "Electrical Properties of Evaporated Aluminum-Oxide Films," J. Electrochemical Soc., Vol. 109, No. 1, January 1962, p. 12.

2. Ryshkewitch, E., Oxide Ceramics, Academic Press, 1960, p. 175.

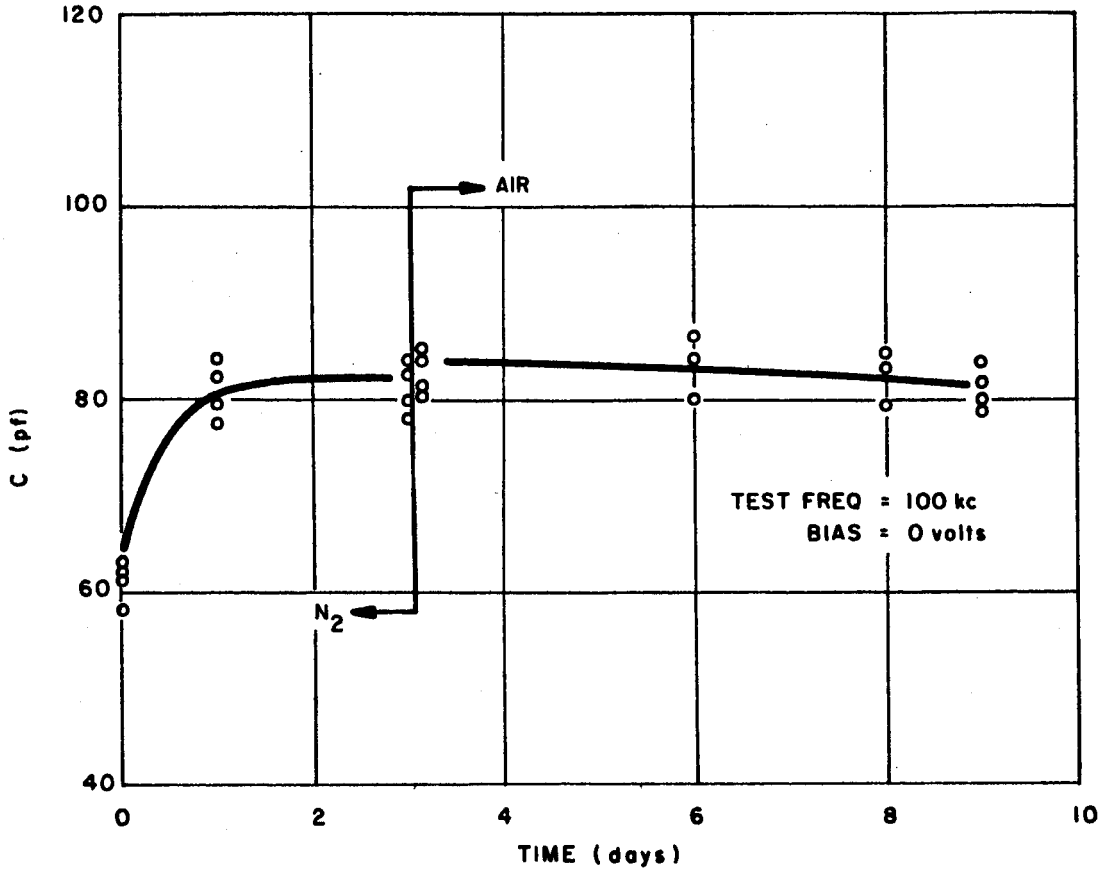

Figure 3. Capacity Versus Time for Run A-1

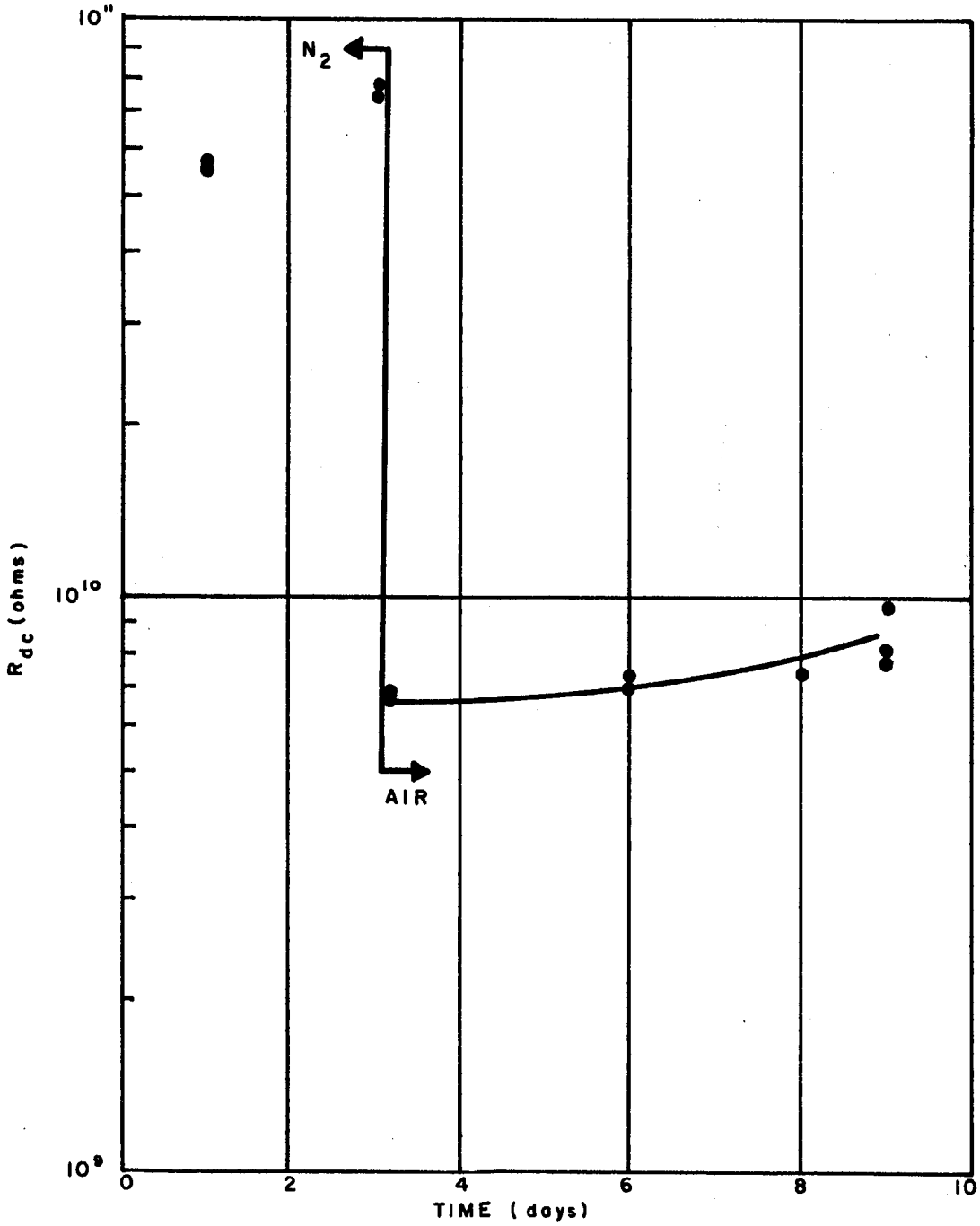

Figure 4. R_{dc} Versus Time for Run A-1

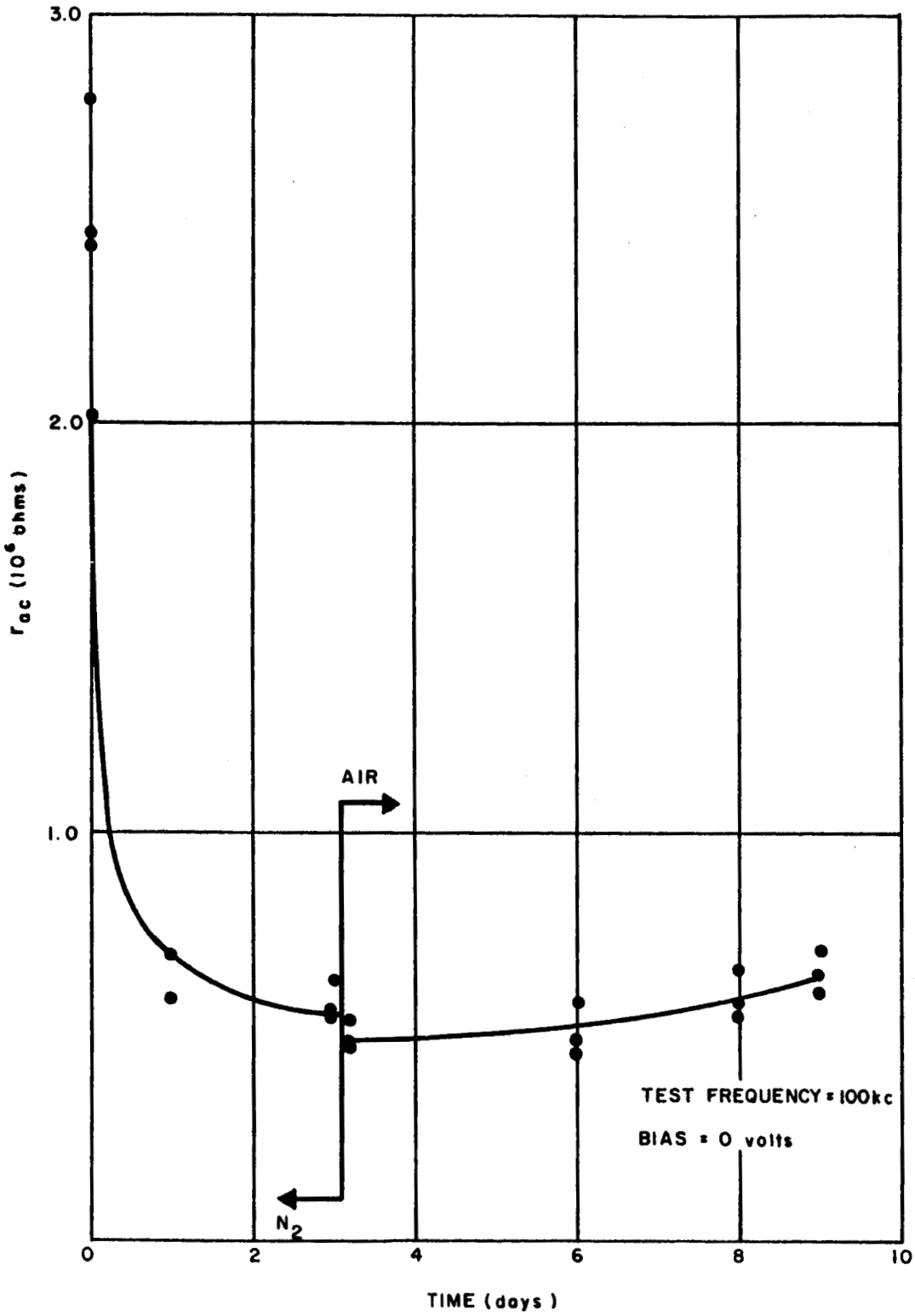

Figure 5. r_{ac} Versus Time for Run A-1

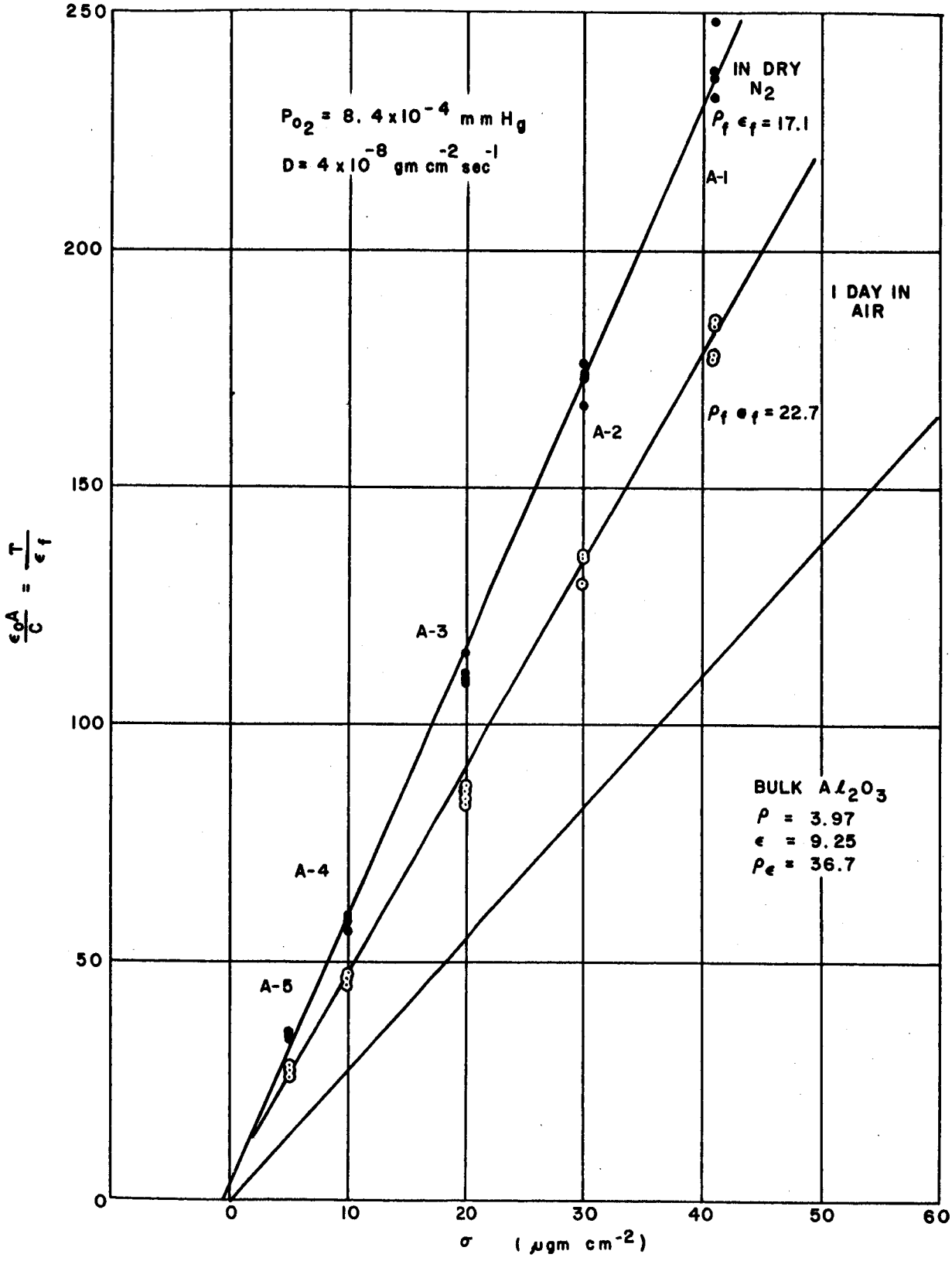

Figure 6. $\frac{T}{\epsilon_f}$ Versus σ for Small-Area Samples

Variation of r_{ac} with σ. - Assuming that the ac loss occurs uniformly within the dielectric and that the loss in the electrodes and leads is negligible, one can relate loss and σ:

$$r_{ac} = \frac{T}{A}\mathscr{R}$$

where

T = Thickness (cm)

A = area (cm^2)

$\mathscr{R}$ = resistivity (Ω cm)

Now,

$$T = \frac{\sigma}{\bar{\rho}} .$$

Therefore,

$$r_{ac} = \frac{\sigma\mathscr{R}}{\bar{\rho}A}$$

or

$$r_{ac}A = \frac{\sigma\mathscr{R}}{\bar{\rho}} .$$

Thus, the slope, m, of $r_{ac}A$ versus σ would be

$$m = \frac{\mathscr{R}}{\bar{\rho}} \text{ for a straight-line fit.}$$

Experimentally, the variation of $r_{ac}A$ with σ (Figure 7) is a straight-line fit if one allows for the variation in r_{ac} produced by the variation of H_2O in the drybox. As an example, an N_2 supply failure prematurely exposed run A-3 (σ = 20 μgm cm^{-2}) to water vapor and thus lowered the r_{ac}. Neglecting the scatter and the nonzero σ intercept, one can calculate m for these films to be

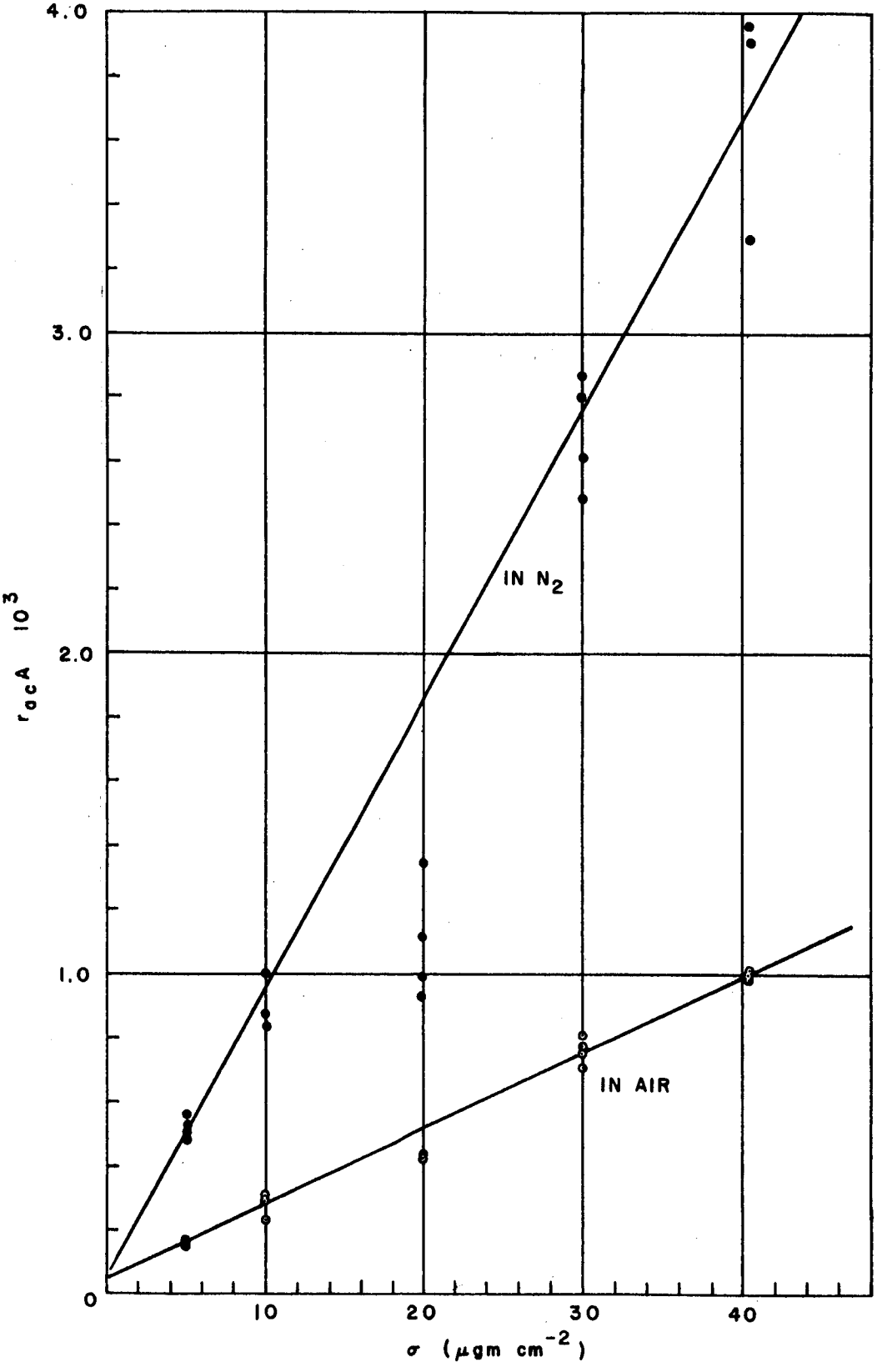

Figure 7. $r_{ac}A$ Versus σ, Small Area, for Runs A-1 to A-5

$$m_{N_2} = \frac{\Delta r_{ac_{N_2}} A}{\Delta \sigma} \approx \frac{4 \times 10^3}{40 \times 10^{-6}} = 10^8 \frac{\Omega \text{ cm}}{\text{gm cm}^{-3}}$$

Therefore,

$$\frac{\mathcal{R}_{N_2}}{\overline{\rho}} = m_{N_2} = 10^8 \frac{\Omega \text{ cm}^4}{\text{gram}} .$$

This compares to bulk Al_2O_3, where

$$\mathcal{R}_{100kc} \gtrsim 10^{10} \Omega \text{ cm}$$

$$\rho = 4.0 \text{ gm cm}^{-3} .$$

Therefore,

$$\frac{\mathcal{R}_{100kc}}{\rho} \geq 2.5 \times 10^9 \Omega \frac{\text{cm}^4}{\text{gram}} .$$

As expected, the thin films are considerably lower. However, it is felt that m is a useful figure of merit when comparing Al_2O_3 films formed under varying conditions. Note that exposure to air drastically reduces r_{ac}. Thus, m_{air} is approximately $2.5 \times 10^7 \Omega \text{ cm}^4 \text{ gram}^{-1}$.

ELECTRON TRANSPORT THROUGH THIN FILMS

Introduction

The basic measurement in this experiment consists of measuring the fraction of incident hot electrons that pass through a thin gold film. Referring to Figure 8, electrons impinge normally on the gold film at an energy $\mathcal{E}$ above the gold Fermi level. An electron that is transported across the film without undergoing a collision (which causes sufficient momentum transfer to divert its trajectory outisde the critical angle) will be transmitted across the gold-silicon interface and contribute to a current at the ohmic contact. Electrons that do collide with scattering sites in the gold will eventually drop down to the Fermi level and appear as current at the gold-film contact. Because of the small transfer ratios expected over much of the range of measurement and the resulting small currents, an area of the gold film as large as possible must be presented to the electron beam. The area of the gold-silicon interface will then also be very great.

Diode Preparation

Material for the diodes was obtained in the form of 0.5-inch-square by 0.020-inch-thick silicon wafers, optically polished on one side. The following steps were then followed for each wafer (refer to Figure 9):

a. Grow thermal oxide to depth of ~ 4000 Å.

b. Sand-blast an area on the cut side of the wafer to remove oxide so that an ohmic contact can be made.

c. Electroless nickel plate on the bared silicon.

d. Evaporate land areas in the form of two chrome-gold stripes onto the oxidized polished side.

e. Mask the land areas with tygon paint and etch off remaining SiO_2 with buffered HF solution (formula). Remove tygon with solvent.

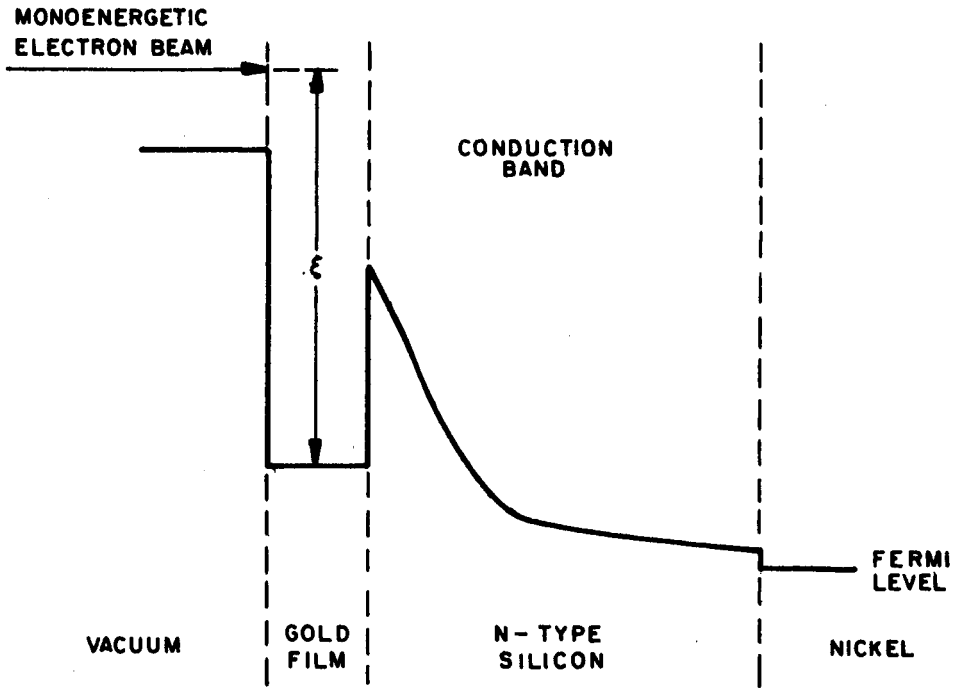

Figure 8. Simplified Energy Diagram of Collector Diode

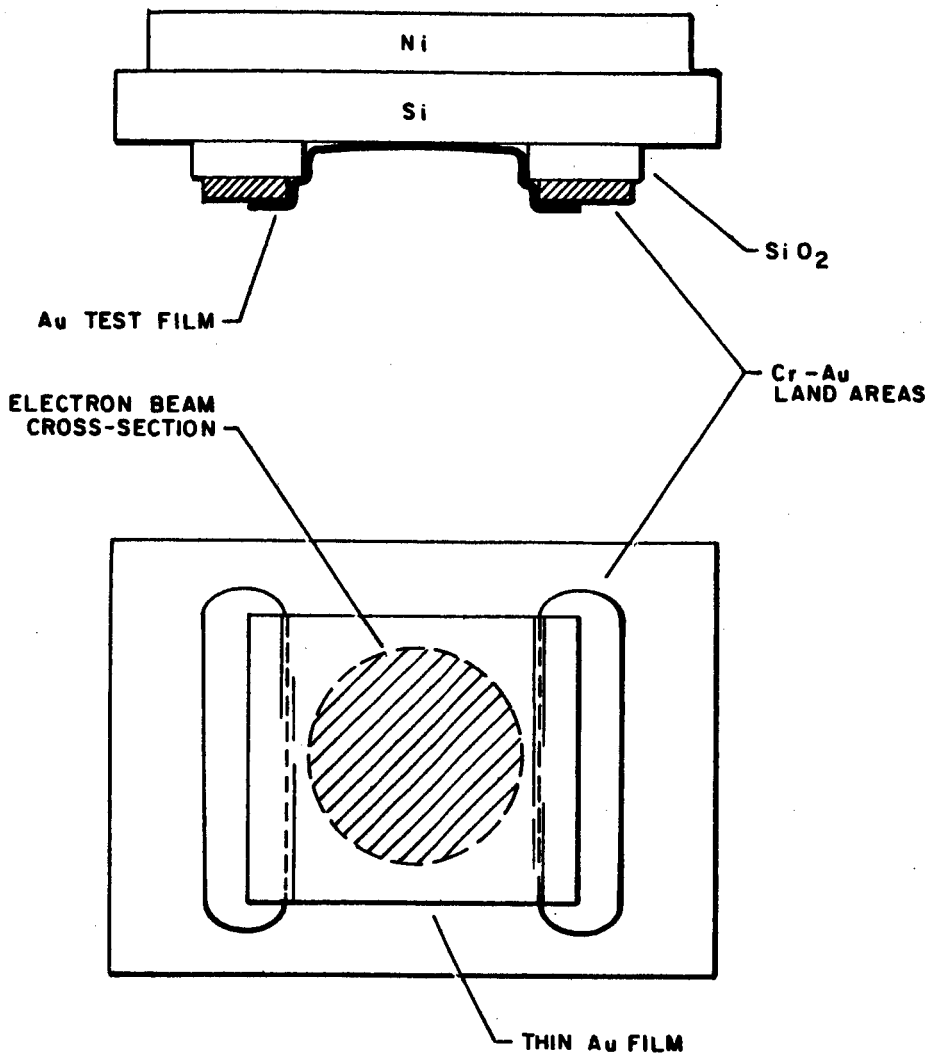

Figure 9. Gold-Silicon Diode

f. Install wafer in high-vacuum system with the electron gun; make electrical connection to ohmic contact and land areas.

g. As part of the measurement run, evaporate thin gold film spanning area between lands.

After step g, the diode can be rotated into alignment with the electron gun for measurements.

The first problem that arose in diode fabrication was the tendency of the land areas to short through the oxide to the silicon. Figure 10 shows an I-V curve for such a diode (made on a Tektronix 575 curve tracer). This difficulty was overcome by having the wafers oxidized at Philco's Lansdale Special Products Division, where facilities exist for doing this work routinely as part of the microminiaturization R and D. It was also found that no cleanup etching could be done before the Cr-Au evaporation if shorts were to be avoided. Figure 11 shows I-V traces of a pair of satisfactory land areas.

Diodes intended for transport measurement could not be tested before installation in the high-vacuum system. The last step in fabrication of the diode (evaporation of the thin gold film) must be done as part of the measurement run (step g, above). A separate diode, not to be used for transport measurements, was completed for the purpose of obtaining diode characteristics. Figure 12 gives the diode I-V curve plotted on a semilog scale to show an exponential forward characteristic. The diode tested has an area of 1.2 cm^2 so that the current scale roughly represents current density in amperes/cm^2. The saturation current density, J_o, of $\sim 5 \times 10^{-3}$ amperes/cm^2 is about three orders of magnitude greater than might be expected for small-area diodes.

Transport Experiment

Attempts made to measure the mean free paths of fast electrons were frustrated by failure to get a beam current from the electron gun. The gun was operated as described in the First Quarterly Report. With positive bias, the focusing tube drew a current of the expected magnitude, or about 0.5 microampere. As the bias was reduced and made negative, the focuser current was reduced, but neither the grid nor the target collected a current. Several attempts were made to discover the reason for this anomalous failure but without success.

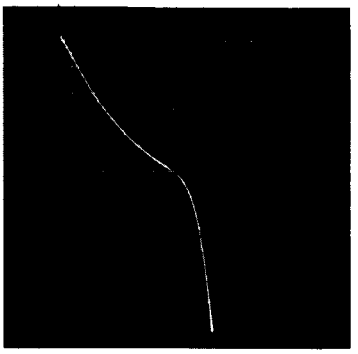

Figure 10. I-V Curve of Au-Si Diode

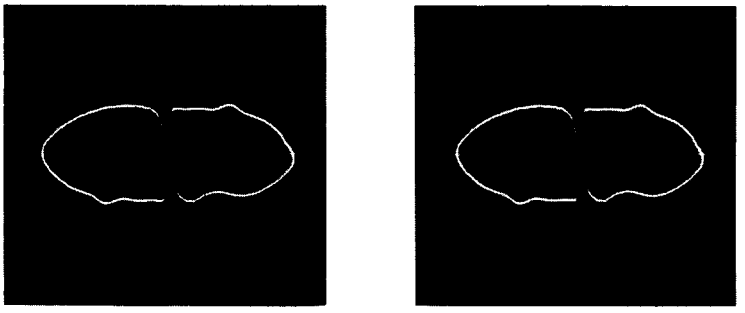

Figure 11. I-V Curves, Showing Isolation of Land Areas From Silicon Surface by SiO_2

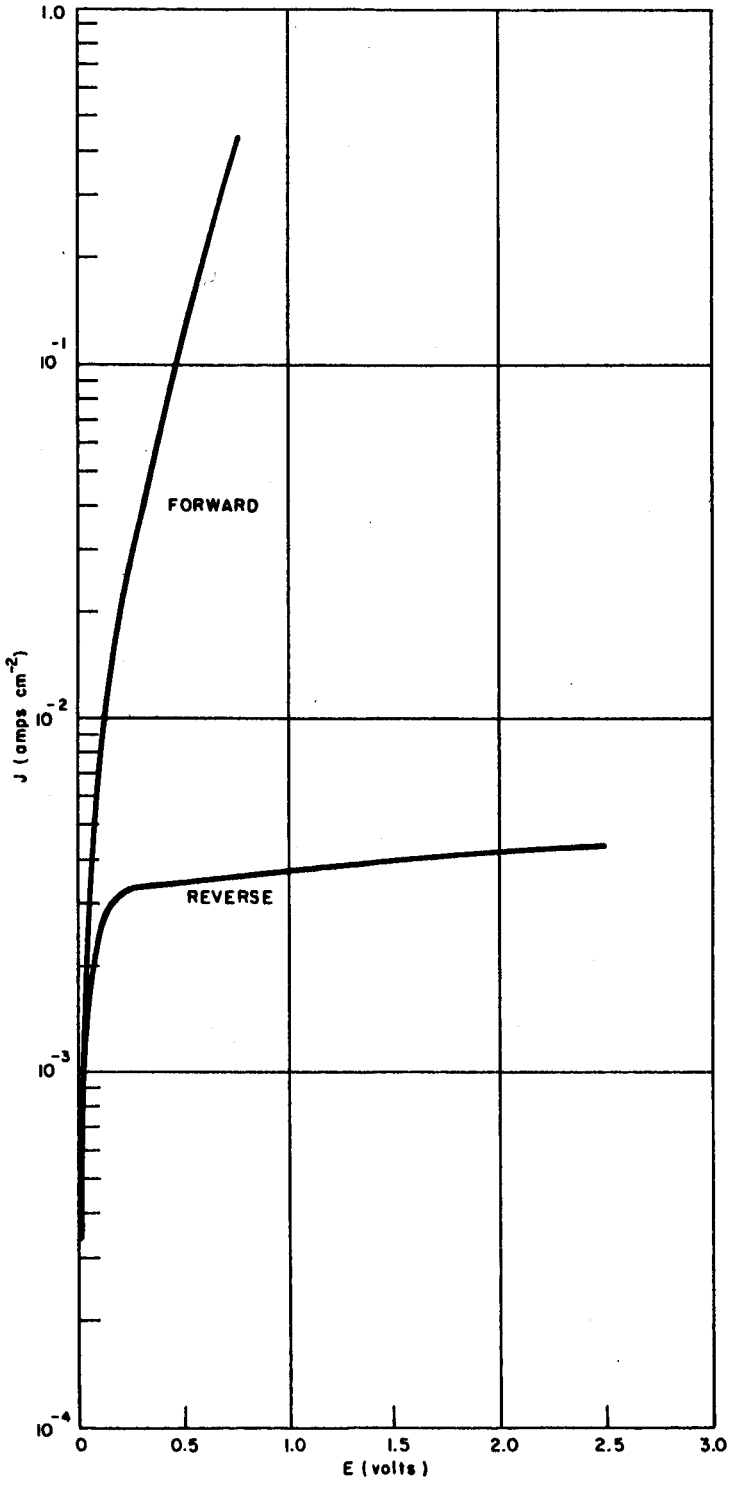

Figure 12. I-V Characteristics of Au-Si Diode

Rather than delay the experiment any further, another gun is being installed in the system. This is a gun which was made previously and is of simpler design. It is smaller and has no grid or shield. It has the disadvantage that an ion current of a few nanoamperes is collected with the target negatively biased, and that there will be a large spurious capacitive coupling to the collector diode.

APPENDIX A

OPERATION AND PERFORMANCE OF THE R. Q. M. DEPOSITION MONITOR AND CONTROLLER

The R. Q. M. deposition monitor and controller can be utilized in two ways: it can monitor a deposition that is manually controlled, or it has the capability of monitoring and controlling the deposition. The system provides continuous records of SURFACE MASS, σ, versus time and of DEPOSITION RATE, D, versus time. Calibration of the σ and D recordings is dependent upon the settings of the various system controls. Table A-1 summarizes the ranges of σ and D that can be accommodated by the system. Note that the time required to deposit σ_o will vary from a minimum of 45.4 seconds for maximum rates to a maximum of 5×10^4 seconds for minimum rates.

Table A-1. Range of Controlled σ and D

f_o (kc)	σ_o (μgm cm^{-2})	D_{min} (gm cm^{-2} sec^{-1})	D_{max} (gm cm^{-2} sec^{-1})
1.0	5.0	1.0×10^{-10}	1.10×10^{-7}
3.16	15.8	3.16×10^{-10}	3.48×10^{-7}
10.0	50.0	1.0×10^{-9}	1.10×10^{-6}
31.6	158.0	3.16×10^{-9}	3.48×10^{-6}
100.0	500.0	1.0×10^{-8}	1.10×10^{-5}

Setting up the System

To set up the R. Q. M., one must first select the Surface Mass and the Deposition Rate desired. A FREQUENCY METER SCALE is then chosen such that the Surface Mass is less than the full-scale limit. One must provide a reasonable excess of scale range to allow for rate stabilization when choosing the FREQUENCY METER SCALE.

$$\Delta f = \frac{\sigma}{S} ,$$

where

σ = surface mass to be deposited, micrograms cm^{-2}

S = system sensitivity, 5 micrograms $kilocycle^{-1}$

$\sigma_o = f_o S.$

Thus, the FREQUENCY METER SCALE, f_o, that is larger than Δf should be chosen.

Having selected a FREQUENCY METER SCALE, the rate-recorder calibration can be calculated using the rate-recorder equation after a selection of the DIFFERENTIATOR MULTIPLIER setting is made. THE DIFFERENTIATOR MULTIPLIER, M_D, setting should be chosen such that the rate-recorder voltage does not exceed 1.0 volt. Except for the highest rates, it is desirable to set the DIFFERENTIATOR MULTIPLIER at "X 1."

$$D = e_d \left[\frac{f_o M_D}{10^5} \right] \mu gm\ cm^{-2}\ sec^{-1}$$

where e_d is the rate voltage as read by the RATE RECORDER. Note that the RATE PROGRAMMER, M_P, and RATE SET, N, controls do not influence the monitoring operation, and both controls should be set at the maximum value when monitoring as this tends to reduce the loading on the differentiator.

For rate-controlled depositions, the settings of the RATE PROGRAMMER and the RATE SET potentiometer are calculated from the deposition rate control equation.

$$D = N f_o M_D M_P \times 10^{-7} \ \mu gm \ cm^{-2} \ sec^{-1}$$

where

N = RATE SET dial reading, 1.0 to 11.0

f_o = frequency meter full-scale reading in cycles 1, 3.16, 10, 31.6, or 100 kc

M_D = DIFF. MULTI. setting, X1 or X10

M_P = PROG. MULTI. setting, X1 or X10

Beginning a Controlled or Monitored Deposition

After one has set the system controls to the values previously calculated and is otherwise prepared to make the deposition, the following procedure is typical of a controlled deposition run.

With the power applied to all equipments, the SERVO MODE switch in "Manual," and the RATE DETECTOR "Off," the EVAPORATOR POWER is switched "On." The MANUAL VARIAC is then used to bring the evaporator structure up to the approximate operating point. Up to this time, a shutter or other suitable structure has protected both the substrate and the sample oscillator from the evaporant. One may now switch the RATE DETECTOR to "On" and open the shutter over the sample oscillator. Assuming that the indicated rate is not at the desired level, the MANUAL VARIAC is further adjusted until the rate is within 20 to 40 percent of the desired rate. The servo variac voltage should be checked at this time to ensure that it is greater than zero and less than maximum, so that the servo system will have sufficient range to control the evaporation. In general, the MANUAL SERVO switch is used to adjust the servo variac for approximately a 30-volt servo variac voltage reading. An initially low value of servo variac voltage is used

since, in the majority of evaporations, the input to the evaporator will increase substantially during the deposition; thus, the servo variac must be initially operated near the minimum voltage level to provide the necessary dynamic range.

Once the deposition rate has been adjusted manually to approximately the desired rate, the SERVO MODE switch can be moved to the "Automatic" position and the servo system will maintain the preset deposition rate by automatically varying the evaporator voltage.

If manual control is to be used, the operator can use the MANUAL "Increase" "Decrease" switch to adjust the evaporation rate to the desired value; if larger changes are required, the MANUAL VARIAC can be used.

Because of the extremely nonlinear relationship between evaporation rate and evaporator voltage, it is usually necessary to provide only a small variation in the total evaporator voltage to produce considerable change in evaporation rate. For this reason, the voltage applied to the evaporator by the servo variac is stepped down in a small multiple-secondary transformer (T_1, Figure C-18, First Quarterly Report). This voltage is essentially in series with the MANUAL VARIAC voltage and provides the small variation in total evaporator voltage needed to control the deposition rate. Quite obviously, the correct transformer taps can be chosen only after one has obtained some knowledge of the particular evaporator and material characteristics being utilized. A selection of transformer tap is most easily made if one first obtains experimentally a curve of deposition rate versus evaporator voltage. One can then select the appropriate transformer tap on the basis of the change in evaporation rate and therefore the change in evaporator voltage required.

Fundamental System Limitations

The system as designed will monitor surface masses up to 500 micrograms per sq. cm. The range of deposition rates that can be controlled is dependent upon the mass range (frequency-meter scale) selected.

The fundamental lower limit on deposition-rate monitoring, and therefore deposition-rate control, is that of system noise. System noise may arise in the random variations in frequency of both the sample oscillator and the reference oscillator. Noise can also be introduced in the

differentiator and in the frequency meter. A slightly different noise is that produced by thermal shocks on the surface of the sample-oscillator crystal. These shocks can be caused by infrared radiation or by localized heating due to chemical reactions on the surface of the crystal. In general, the major limitations on system performance are those of sample-oscillator frequency stability and the noise introduced by the frequency meter. Experimentally, the sample-oscillator noise is equivalent to 8×10^{-11} grams cm^{-2} sec^{-1}. Frequency-meter noise arises almost entirely in the dc power-supply fluctuations which produce output noise proportional to the output current. Thus, this noise is a function of the scale reading. Experimentally, this noise has been determined to be $\sigma_o \times 10^{-11}$ grams cm^{-2} sec^{-1}, where σ_o is the full-scale surface mass. The deposition rate range has been chosen such that the minimum deposition rate is only slightly larger than the noise limit for all surface mass ranges. Usually, one should not attempt controlled depositions at rates near the noise limit.

If it is desired to deposit at the lowest possible rate for an extended period of time, the long-term drift of the sample and reference oscillators (resulting from temperature changes) becomes important. DC drift in the frequency meter may also produce errors for very long evaporations.

The maximum controlled deposition rate is most severely limited by the very long response times of most evaporator structures. It is necessary to allow sufficient time for the system to come to equilibrium when performing a rate-controlled evaporation; at high rates, the full-scale surface-mass range can easily be exceeded before equilibrium is obtained.

When monitoring the rate, the aforementioned limit does not apply. In this case, the maximum rate is limited by the transient response of the frequency meter and overload of the differentiator. The frequency-meter intrinsic response constant, τ_f (according to the manufacturer), is $\approx 5 \times 10^{-3}$ second; however, additional filtering required by the rate control electronics increases this value to $\approx 4 \times 10^{-2}$ second. Thus, for a 1-percent or less error, the time of deposition should be greater than 0.3 second. However, the rate for full-scale σ changes cannot be monitored in less than 5 seconds because of the 10-volt limit on the output swing of the operational amplifier. Thus, if rate data is desired, the evaporation time should be in excess of 5 seconds.

ABSTRACT

This report describes experimental work on two areas of study regarding the production of radiation-resistant thin-film active devices.

The experimental determination of electron mean free path in metal films has been severely hampered by the problems in electron gun design and the difficulty with shorts in the large-area surface-barrier collector diodes.

Reactively evaporated aluminum-oxide films with reasonable dielectric properties have been produced over the thickness range from 10 to 40 $\mu gm\ cm^{-2}$. The electrical properties of this oxide layer are sensitive to the ambient gas.